

Electronic Supplementary Information

Na_{0.35}MnO₂ as an ionic conductor with randomly distributed nano-sized layers

Arturas Adomkevicius, Laura Cabo-Fernandez, Tzu-Ho Wu, Tzu-Man Ou, Ming-Guan Chen, Yuri Andreev, Chi-Chang Hu* and Laurence J. Hardwick**

Arturas Adomkevicius, Dr. Laura Cabo-Fernandez, Dr. Tzu-Ho Wu, Prof. Laurence J. Hardwick*

Stephenson Institute for Renewable Energy,
Department of Chemistry
University of Liverpool
Chadwick Building, Peach Street
Liverpool, L69 7ZF, United Kingdom
E-mail: hardwick@liverpool.ac.uk

Arturas Adomkevicius, Dr. Tzu-Ho Wu, Tzu-Man Ou, Ming-Guan Chen, Prof. Chi-Chang Hu*

Department of Chemical Engineering,
National Tsing Hua University,
Hsin-Chu, 30013 Taiwan.
E-mail: cchu@che.nthu.edu.tw

Dr. Yuri Andreev*
School of Chemistry,
University of St Andrew
St Andrews, KY16 9ST
Scotland, United Kingdom
E-mail: ya@st-andrews.ac.uk

Contents

1. Elemental analysis.....	3
2. Powder X-ray diffraction analysis	4
3. Brunauer – Emmett – Teller characterisation	5
4. Transmission electron microscopy and Raman spectroscopy.....	6
5. Electrochemical characterisation	8
6. X-ray absorption spectroscopy.....	9
7. References	11

1. Elemental analysis

The chemical composition of the compound was determined as $\text{Na}_{0.35}\text{MnO}_2$ by elemental analysis via inductively coupled plasma optical emission spectroscopy (ICP-OES) (see Table S1).

Table S1. Elemental analysis of $\text{Na}_{0.35}\text{MnO}_2$ by Inductively Coupled Plasma Optical Emission Spectroscopy (ICP-OES).

Sample	Na wt%	Mn wt%	Formula
A - Na_xMnO_2	8.81	59.53	
B - Na_xMnO_2	8.71	60.17	$\text{Na}_{0.35}\text{MnO}_2$ *
C - Na_xMnO_2	8.69	58.72	

* Calculated Na content in sample A - Na_xMnO_2 is $\text{Na}_{0.354}\text{MnO}_2$; B - Na_xMnO_2 is $\text{Na}_{0.346}\text{MnO}_2$ and C - Na_xMnO_2 is $\text{Na}_{0.354}\text{MnO}_2$ giving an average Na content in the compound of $\text{Na}_{0.35}\text{MnO}_2$.

2. Powder X-ray diffraction analysis

A pattern of an empty, 0.7 mm in diameter, glass capillary was collected first. The powder was placed into the same capillary for the data collection. Both patterns were collected for 25 hours with continuously moving detector. The data were recorded with the step size 0.0167° in 2θ .

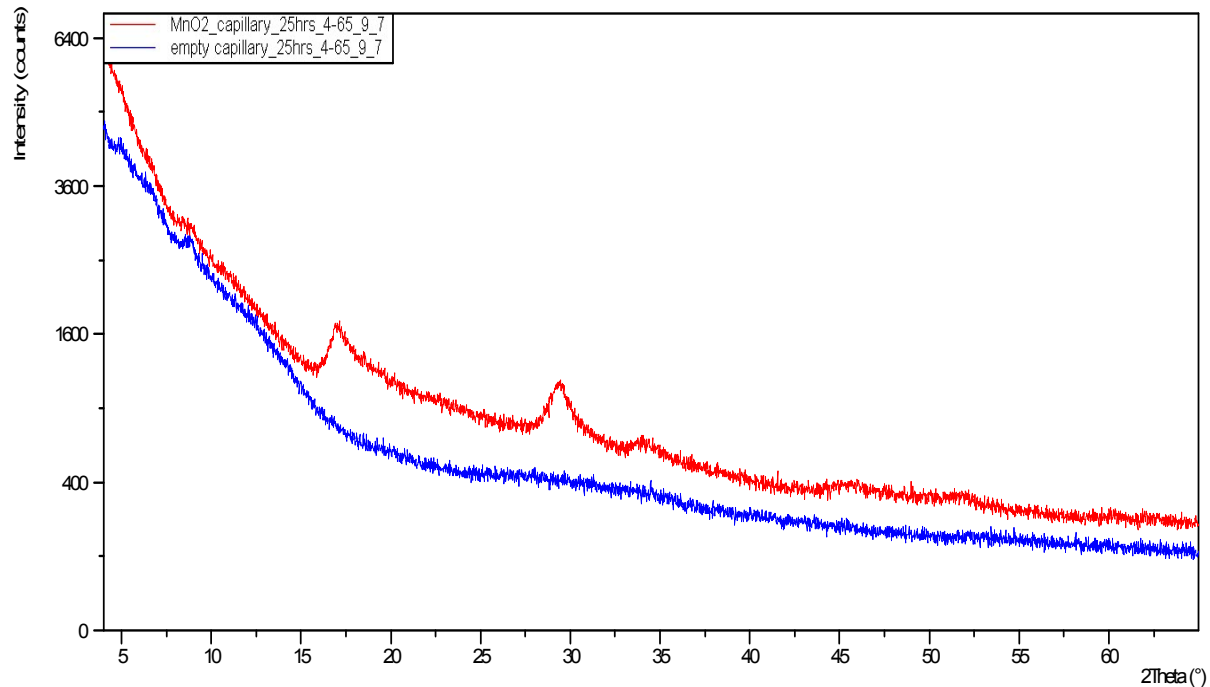


Fig. S1. X-ray diffraction patterns of empty capillary (blue) and the same capillary filled with $\text{Na}_{0.35}\text{MnO}_2$ (red)

In the course of refinement the pattern from empty capillary was added to the profile calculated using the equation of Debye.

3. Brunauer – Emmett – Teller characterisation

The surface area of $\text{Na}_{0.35}\text{MnO}_2$ was found to be $15 \text{ m}^2/\text{g}$ (Table S2 and Figure S2). $\text{Na}_{0.35}\text{MnO}_2$ is therefore a 2D ordered material with low porosity, whereby the capacitance is entirely pseudocapacitive.

Table S2. Surface area and pore volume of $\text{Na}_{0.35}\text{MnO}_2$.

Material	Surface area ($\text{m}^2 \text{ g}^{-1}$)	Mesopores volume (cc g^{-1})	Micropores volumes (cc g^{-1})
As-prepared $\text{Na}_{0.35}\text{MnO}_2$	15	0.0593	0.00017

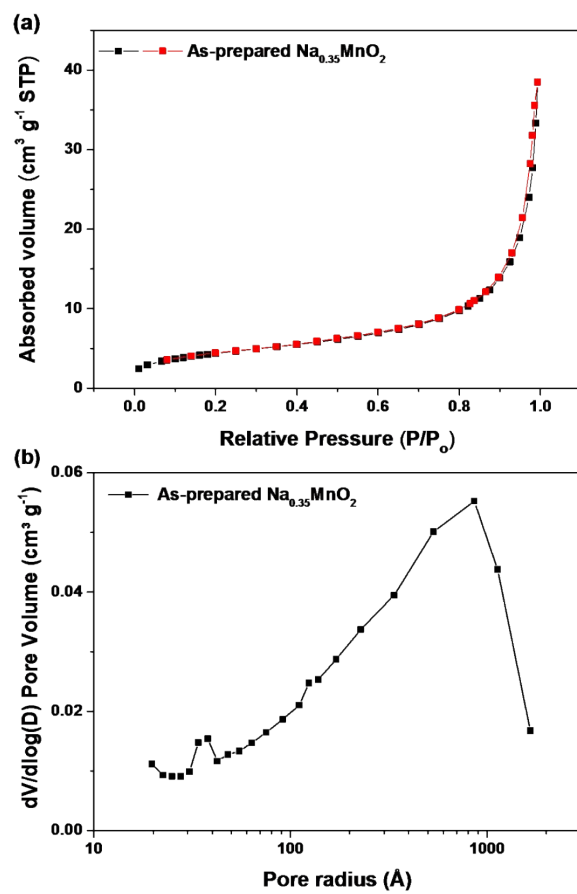


Fig. S2. (a) Nitrogen adsorption/desorption isotherms and (b) pore size distribution curves of Na_{0.35}MnO₂.

4. Transmission electron microscopy and Raman spectroscopy

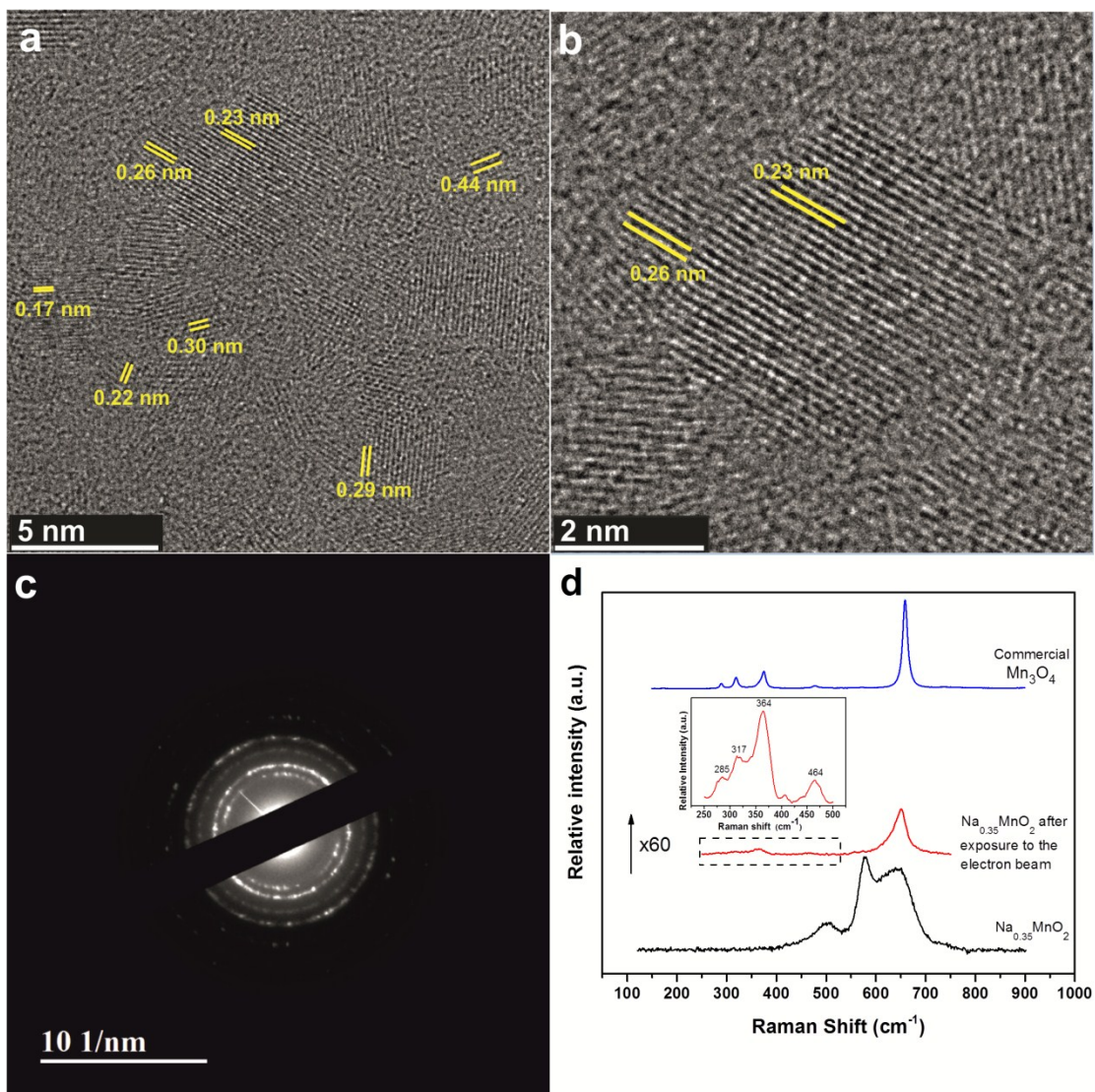


Fig. S3. (a-b) HRTEM images of the as-prepared $\text{Na}_{0.35}\text{MnO}_2$ after exposure to electron beam under high magnification (x800 k) show the transformation to Mn_3O_4 hausmannite phase; (c) selected area electron diffraction (SAED) pattern; (d) Raman spectra of $\text{Na}_{0.35}\text{MnO}_2$ before and after exposure to the electron beam.

Table S3. Comparison of d-spacing of as-prepared $\text{Na}_{0.35}\text{MnO}_2$ after exposed to HRTEM electron beam to hausmannite- Mn_3O_4 JCPDS 75-1560 card from database.

	d-spacing calculated from HRTEM images (nm)	d-spacing hausmannite- Mn_3O_4 database (nm)
$\text{Na}_{0.35}\text{MnO}_2$		0.6159
	0.44	0.4070
		0.3645
		0.3395
	0.30	0.3079
	0.29	0.2929
		0.2877
	0.26	0.2607
		0.2377
	0.23	0.2355
	0.22	0.2258
	0.17	0.1697

5. Electrochemical characterisation

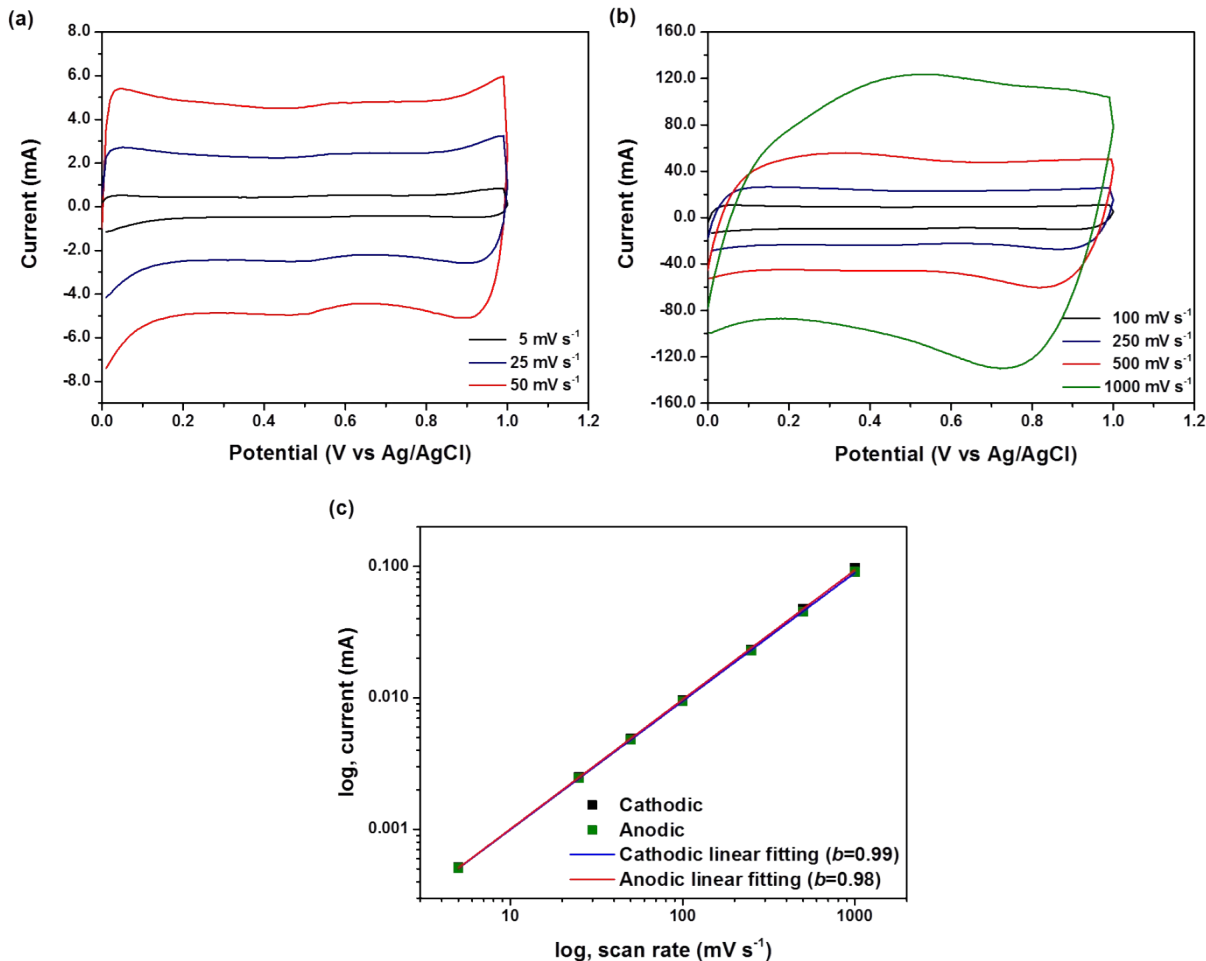


Fig. S4. **(a, b)** Cyclic voltammograms of $\text{Na}_{0.35}\text{MnO}_2$ measured at **(a)** 5 – 50 mV s^{-1} , **(b)** 100 – 1000 mV s^{-1} ; **(c)** logarithmic plots of cathodic and anodic current of $\text{Na}_{0.35}\text{MnO}_2$ electrode versus scan rates between 5 – 1000 mV s^{-1} in 0.5 M Na_2SO_4 (for sweep rates ranging from 5 to 1000 mV s^{-1} , the linear fitting b -value (slope) for both the cathodic (0.99) and anodic (0.98) average currents is close to 1 indicating that high rate capability is due to fast kinetics which is predominantly surface-controlled.¹⁾

6. X-ray absorption spectroscopy

Beamline B18 of Diamond Light Source. The Si(111) double crystal was used to monochromatise the X-ray photon energy. The samples were prepared into 13 mm pellets and measured in transmission mode. The XAS energy was calibrated using the first inflection point of Mn K-edge region of a metallic Mn foil (6539 eV) recorded simultaneously in each scan.

Manganese oxides with different oxidation states (MnO , Mn_3O_4 , Mn_2O_3 and MnO_2 from Sigma-Aldrich without any further treatment) are used as standard materials to create a quasi-linear relationship between Mn K-edge energy and Mn oxidation state.

Table S4. The Mn oxidation state of manganese oxides

Sample	Mn K-edge Energy [eV]	Mn Oxidation state	Reference
Standard samples			
MnO	6544.21	2	
Mn_3O_4	6547.08	2.67	$R^2=0.9996$
Mn_2O_3	6548.42	3	
MnO_2	6552.34	4	
Na-doped MnO_x Samples			
As-prepared $\text{Na}_{0.35}\text{MnO}_2$	6550.52	3.57	
$\text{Na}_{0.35}\text{MnO}_2$ after 100 cycles	6550.37	3.54	This work
$\text{Na}_{0.35}\text{MnO}_2$ after 1200 cycles	6550.02	3.45	
Literature			
MnO	6544.7	2	
Mn_2O_3	6548.2	3	⁶
MnO_2	6552.6	4	
MnO	~6545.75	2	
Mn_2O_3	~6547.75	3	
LiMn_2O_4	~6548.75	3.5	⁷
MnO_2	~6549.75	4	

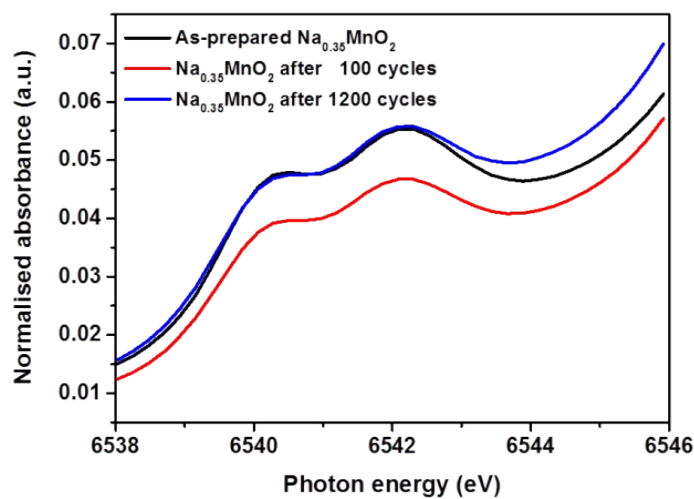


Fig. S5. The X-ray absorption near-edge structure (XANES) spectra of $\text{Na}_{0.35}\text{MnO}_2$.

7. References

- 1 V. Augustyn, J. Come, M. A. Lowe, J. W. Kim, P.-L. Taberna, S. H. Tolbert, H. D. Abruña, P. Simon and B. Dunn, *Nat. Mater.*, 2013, **12**, 518-522.
- 2 C. Julien, M. Massot, R. Baddour-Hadjean, S. Franger, S. Bach and J. P. Pereira-Ramos, *Solid State Ion.*, 2003, **159**, 345-356.
- 3 D. Chen, D. Ding, X. Li, G. H. Waller, X. Xiong, M. A. El-Sayed and M. Liu, *Chem. Mater.*, 2015, **27**, 6608-6619.
- 4 Y. K. Hsu, Y. C. Chen, Y. G. Lin, L. C. Chen and K. H. Chen, *Chem. Commun.*, 2011, **47**, 1252-1254.
- 5 Z. Su, C. Yang, B. Xie, Z. Lin, Z. Zhang, J. Liu, B. Li, F. Kang and C. P. Wong, *Energy Environ. Sci.*, 2014, **7**, 2652-2659.
- 6 J. K. Chang, M. T. Lee and W. T. Tsai, *J. Power Sources*, 2007, **166**, 590-594.
- 7 K. W. Kim, M. G. Kim and K. B. Kim, *J. Phys. Chem. C.*, 2007, **111**, 749-758.